PREDICTION OF STRAIN RATE SENSITIVITY OF POLYMERS FROM INTEGRAL TRANSFORM OF DYNAMIC MECHANICAL DATA

THESIS

Submitted in Partial Fulfillment of

the Requirements for

the Degree of

MASTER OF SCIENCE (M.E.)

at the

NEW YORK UNIVERSITY
TANDON SCHOOL OF ENGINEERING

by

Steven Eric Zeltmann

January 2017

PREDICTION OF STRAIN RATE SENSITIVITY OF POLYMERS FROM INTEGRAL TRANSFORM OF DYNAMIC MECHANICAL DATA

THESIS

Submitted in Partial Fulfillment of

the Requirements for

the Degree of

MASTER OF SCIENCE (M.E.)

at the

NEW YORK UNIVERSITY
TANDON SCHOOL OF ENGINEERING

by

Steven Eric Zeltmann

January 2017

Approved:

Advisor Signature

Date

Department Chair Signature

Date

University ID: N18278428

Net ID: sez237

VITA

July 28, 1994 ..... Born: Garden City, New York

September 2012 to Present ..... B.S./M.S, Mechanical and Aerospace Engineering, NYU Tandon School of Engineering, Brooklyn, New York

Fields of Study:

B.S. Major ..... Mechanical Engineering

B.S. Minor ..... Aerospace Engineering

M.S. Major ..... Mechanical Engineering

M.S. Specialty ..... Mechanics and Structural Systems

Employment:

May 2013 to present ..... Research Assistant, Composite Materials and Mechanics Laboratory, NYU Tandon

Summer 2015 & 2016 ..... Assistant Instructor, Engineering Division, NYU Abu Dhabi

ACKNOWLEDGEMENTS

I would like to first thank my advisor, Dr. Nikhil Gupta, for his support of this project and of my budding career as a researcher. My lab colleagues, particularly Brian Chen and Chrys Koomson, have contributed greatly to the success of this work by assisting in performing experiments and processing data. William Peng has also substantially aided this work through numerous helpful mathematical discussions.

This work was supported by the Office of Naval Research grant N00014-10-1-0988. The views expressed in this article are those of the author, not of the funding agencies. Dr. Mrityunjay Doddamani of NIT-K, Surathkal, India is thanked for providing some of the samples for study. MAE Department at NYU and Engineering Division at NYUAD are also thanked for providing facilities and support.

ABSTRACT

PREDICTION OF STRAIN RATE SENSITIVITY OF POLYMERS FROM INTEGRAL TRANSFORM OF DYNAMIC MECHANICAL DATA

by

Steven Eric Zeltmann

Advisor: Prof. Nikhil Gupta, Ph.D.

Submitted in Partial Fulfillment of the Requirements for

the Degree of Master of Science (M.E.)

January 2017

Recent interest in understanding the effect of strain rate on mechanical properties has motivated this study to develop a correlation between frequency domain dynamic mechanical analysis (DMA) results and elastic modulus values that are obtained from a separate set of elaborate tensile tests conducted over a wide range of strain rates. Using the time-temperature superposition principle and the integral relations of viscoelasticity, the DMA results are converted into a time-domain relaxation function in order to predict the strain-rate dependent modulus. To confirm the validity of this approach, results on HDPE, HDPE/fly ash composites, and vinyl ester are compared with the predictions from DMA transform and found to be in

good agreement over a wide range of strain rates. An estimate of the range of strain rates for which the method is applicable is obtained. Cross correlation between DMA results and tensile test results over a wide range of strain rates can help in substantially reducing the requirement for tests that are needed to characterize the material behavior with respect to strain rates, temperature and loading frequency. The procedure is briefly illustrated in the graphical abstract below, which shows a set of DMA frequency sweeps at varying temperature and the resulting prediction of strain rate sensitivity for high density polyethylene [1].

TABLE OF CONTENTS

LIST OF FIGURES

LIST OF TABLES

CHAPTER 1. INTRODUCTION

Despite the wide availability of dynamic mechanical analysis (DMA) results on polymers and polymer matrix composites, such data have rarely been applied to design of structures and components because frequency-domain results obtained through this method are not directly applicable to most engineering problems. For thermosets, dynamic mechanical analysis is principally used to find maximum use temperature and glass transition temperature (T_g) [2, 3], which can determine the suitability of the material for application in a particular environment. However, for thermoplastics which are used above T_g, such as high density polyethylene (HDPE), and whose mechanical response is highly time-dependent, such information is less useful.

The storage and loss moduli obtained from DMA provide a measure of energy stored and lost, respectively, in a material when a cyclic loading-unloading profile is applied. Numerous DMA studies on polymers can be found. DMA is considered the most sensitive method to locate thermal transitions [4-8] including those in crystallization and resin curing. When combined with other spectroscopy methods, information from DMA can reveal activation of different modes of motion of the polymer chains [9-11]. DMA is also used to gain information on the temperature sensitivity of the behavior of polymer blends [12, 13], pharmaceutical and biomedical materials [14], and micro- [15-17] and nano-composites [18-26]. Most of these studies have reported storage modulus *E'*, loss modulus *E"*, damping parameter tan δ, and T_g. However, the relation of *E'* and *E"* to elastic modulus at different strain rates is not developed in these studies, which is a major current limitation in using the DMA results in mechanical design. In order to develop this relation, the DMA data needs to be transformed into a time-

domain representation which can yield more readily useful information about the material behavior.

Measurement of properties at widely varying strain rates is often complicated by the limited crosshead displacement speed ranges attainable within one testing setup or by a particular method. In addition, very low strain rate tests are time consuming and expensive to conduct, making it difficult to test multiple specimens at multiple strain rates and temperatures to develop a comprehensive understanding of mechanical properties of the material. Augmenting these present limitations, it is also noted that the correlation between results obtained from tensile or compressive tests with DMA results have not been established to develop a comprehensive understanding of the time and temperature dependent behavior of materials.

In this work, the frequency-domain storage modulus function obtained by DMA is inverted to obtain the time-domain relaxation function, which is then used to obtain the linear viscoelastic response of the materials at a given strain rate. Various material properties can be found from this transformed data, such as secant (or tangent) modulus at a given strain, and energy absorption at a given elastic strain. Various exact and approximate relations exist for converting this function to creep compliance as well [27, 28]. Using the time-temperature superposition (TTS) principle, a series of frequency sweeps at different temperatures are combined to yield the isothermal frequency response over a frequency range that is wide enough to ensure convergence of the transform over the desired strain rates. This transform technique is validated by comparing the predictions with reported values for HDPE in the literature and good agreement is found over a wide range of strain rates. HDPE was chosen for study in this work due to its widespread use in manufacturing industrial products. HDPE is

also used extensively as a matrix resin in polymer matrix composites [29, 30]. However, the method developed in this work is expected to be applicable to other polymers as well.

Hollow particle filled composites called syntactic foams are lightweight materials that are used in structural applications due to their excellent specific compressive strength and stiffness [31]. The existing applications of these materials include underwater vehicle structures, submarine buoyancy modules, buoys, aircraft parts, and thermoforming plugs [32]. Most of the existing studies on syntactic foams are available on epoxy and vinyl ester matrices. In comparison, studies on thermoplastic matrix syntactic foams are scarce as summarized in chapters of a recent book [33, 34]. Low and high density polyethylene (LDPE and HDPE), polymethyl methacrylate, and polylactic acid [35, 36] are among the thermoplastic resins that are widely used in fabricating consumer products. Use of these resins in fabricating syntactic foams can provide opportunities of saving weight in existing applications and also in developing new applications. One of the advantages of using thermoplastic resins is the possibility of using rapid manufacturing industrial techniques for making syntactic foam parts. Therefore, it is of great interest to develop and study thermoplastic resin syntactic foams.

Hollow glass particles and cenospheres have been used as fillers in syntactic foams. Fly ash, an industrial waste material generated in coal fired power plants, contains hollow particles called cenospheres [37, 38]. Alumina and silica are the main constituents of cenospheres, which have higher mechanical properties than glass [39]. Use of such industrial waste material can help in addressing the fly ash disposal and also in creating high performance syntactic foams [40-42]. Cenosphere reinforced thermoset composites are widely investigated in the literature for structural applications [43-46]. The present work uses

fly ash cenospheres for developing syntactic foams. These particles have numerous defects present in their walls and are not perfectly spherical, which compromises their properties compared to engineered particles with perfect walls and spherical shape. The alumino-silicate composition of cenospheres compensates for the loss in mechanical properties due to the presence of defects and their properties are generally in the range observed for the commonly used glass microballoons [46].

Several challenges can be identified related to thermoplastic syntactic foams based on the existing observations. While use of high volume fraction of hollow particles can provide lower density syntactic foams, most of the current literature has studied thermoplastic syntactic foams with up to 20 wt.% particles. The available studies on thermoplastic syntactic foams process materials under controlled conditions at laboratory scale, which usually provides syntactic foams with high quality. However, processing of materials with industrial scale manufacturing equipment may not yield similar quality so the effect of such manufacturing environment needs to be studied, which is the focus of the present work. Rapid manufacturing is a key to satisfying the ever growing demands of useful and durable products. The present work deals with utilization of one such technique, injection molding, with optimized temperature and pressure to synthesize syntactic foams.

In addition to the HPDE and HDPE/fly ash materials, vinyl ester resin is also examined. Vinyl ester is a thermoset resin with widespread applications as a structural material, especially in composites [3, 31, 44]. The viscoelastic properties of vinyl ester/glass hollow particle syntactic foams have been extensively investigated [3] and TTS data have already

been obtained for a wide swath of composite formulations. This data is useful in the method presented in the present work, as it is sufficient to obtain strain rate sensitivity predictions.

This work is structured in four following chapters. In the Experimental Procedure, the experiments used to obtain DMA and tensile data are described. The material systems and composite fabrication are also briefly covered, and more information on these processes can be found in the literature. In the Results chapter, the experimental measurements taken from dynamic mechanical analysis are presented and TTS is carried out. In the Conversion to Time Domain chapter, the theory behind the method is explained and the steps are shown in detail for one material system. Finally, in the Discussion chapter, the transformation technique is applied to the material systems selected for study in this work and the predictions are compared with the available experimental data.

CHAPTER 2. EXPERIMENTAL PROCEDURE

2.1. Materials

Virgin HDPE of HD50MA180 grade procured from Reliance Polymers, Mumbai, India is studied in the present work. The HDPE has a melt flow index of 20 g/10 min (190°C/2.16 kg). The resin is in granular form of 3 mm diameter and has a mean molecular weight of 97,500 g mol^{-1}. Fly ash cenospheres (CIL-150 grade) supplied by Cenosphere India Pvt. Ltd. Kolkata, India are used as the filler. Both the matrix and filler are used in as-received condition, without any surface treatment. Chemical, physical and sieve analysis of the cenospheres are given in previous work [47] (see Table 1 in the reference). Alumina, silica, calcium oxide and iron oxides are the primary constituents in cenospheres. Particle size and shape analysis is conducted using a Sympatec (Pennington, NJ) QICPIC high speed image analysis system as discussed in earlier work [47].

Vinyl ester (US Composites) cured with methyl ethyl ketone peroxide (MEKP) at 1 vol.% was cast into aluminum molds. The mixture was cured for 24 hours at room temperature and further post-cured at 90 °C for 2 hours.

2.2. Material Preparation

HDPE and HDPE/flyash specimens were fabricated using an industrial scale horizontal type polymer injection molding (PIM) machine (Windsor, 80 ton capacity). Operating and processing parameters of the PIM machine were optimized in a set of earlier studies [29, 30, 48, 49] and are set at 160°C temperature and 30 kg/cm^2 (2.9 MPa) pressure. Samples of dimensions 35×12.7×3.3 mm^3 (length×width×height) were molded for use in the DMA study. Cenospheres are pre-mixed mechanically with neat resin (HDPE) in 20 and 40 weight % and

loaded into the hopper of the PIM machine. The syntactic foams are denoted by “HDPE” followed by the weight percentage of cenospheres, e.g. “HDPE20.”

2.3. Dynamic Mechanical Analysis

Dynamic mechanical analysis is conducted using a TA Instruments (New Castle, DE) Q800 DMA. Specimens of nominal dimensions 35×12.7×3.3 mm^3 were tested in the dual cantilever configuration with a span length of 35 mm. Testing was conducted in the strain control mode with a maximum displacement of 25 μm.

DMA testing was conducted in two phases: (a) using the temperature sweep mode at constant frequency and (b) using the frequency sweep mode at constant temperature. In the temperature sweep test, the temperature is ramped at a rate of 1°C/min with the deformation occurring at a constant frequency of 1 Hz. The temperature range of the testing is different for different materials: testing was begun at -100 °C and was halted once *E’* reached a value of 20 MPa to prevent total melting of the specimen inside the DMA chamber. Liquid nitrogen cooling was used to achieve subambient test temperatures. At least five specimens of each type were tested in this phase. In the frequency sweep testing, the temperature is stepped from -10°C to 120°C in increments of 5°C. At each temperature step the specimen is soaked for 8 minutes to ensure thermal equilibrium. The dynamic properties are measured at 20 discrete frequencies logarithmically spaced between 1 and 100 Hz at each temperature step. At least three specimens of each type were tested in this phase. The results of temperature and frequency sweeping are combined using the time-temperature superposition (TTS) principle to generate master curves describing the behavior of the material over a wider range of frequencies.

2.4. Tensile Testing

Specimens for tensile testing were fabricated according to ASTM D638 for HDPE and HDPE/fly ash syntactic foams. The specimens were fabricated by injection molding into appropriate molds. Parameters for the injection molding process were as optimized in [30]. Specimens of PMMA were fabricated according to the dimensions in ASTM D638 by laser cutting the specimens from a 1/8” thick sheet (Canal Plastics Center, New York, New York) using an ILS 75W laser cutter. Tensile testing of the specimens was conducted using an Instron 4469 universal test frame with a 30kN load cell. An Instron 1” gage length extensometer was used to measure strain in the specimen. The test speed was set to achieve initial strain rates from 10^{-5} to 10^{-2} s^{-1}.

CHAPTER 3. RESULTS

3.1. High Density Polyethylene (HDPE)

3.1.1. Temperature sweep

A representative set of results of the temperature sweep for *E′*, *E″*, and tan δ for one HDPE specimen are shown in Figure 1. As T_g of the HDPE is about -110 °C [50], the experiments in the present work are conducted in the rubbery region and the dynamic properties with respect to temperature do not show step changes or peaks which may indicate phase transitions. Results on *E'* are extracted at three arbitrarily selected temperatures in the rubbery plateau region of 60, 80 and 100 °C and are presented in Table 1.

Table 1. Comparison of dynamic mechanical analysis results at three representative arbitrarily selected temperatures.

Property	60 °C	80 °C	100 °C
E' (MPa)	572.88±4.1	292.59±3.7	135.53±3.4
E" (MPa)	115.05±0.9	70.63±0.7	38.43±0.9
tan δ ($\times 10^{-2}$)	20.08±0.07	24.14±0.19	28.35±0.32

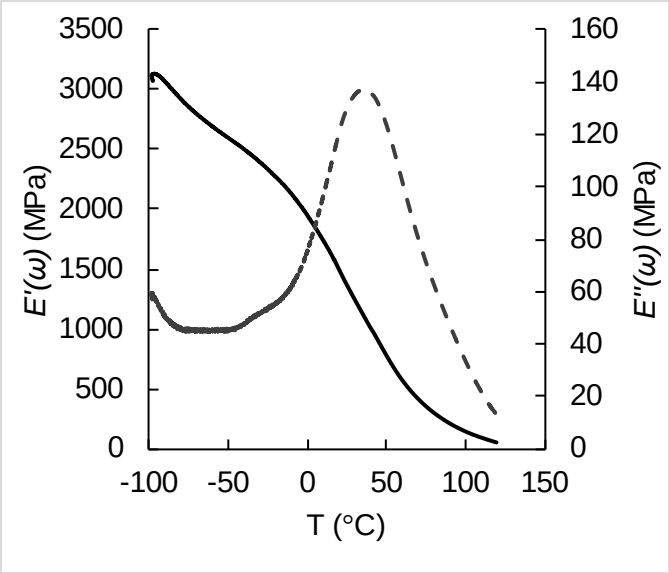

(a)

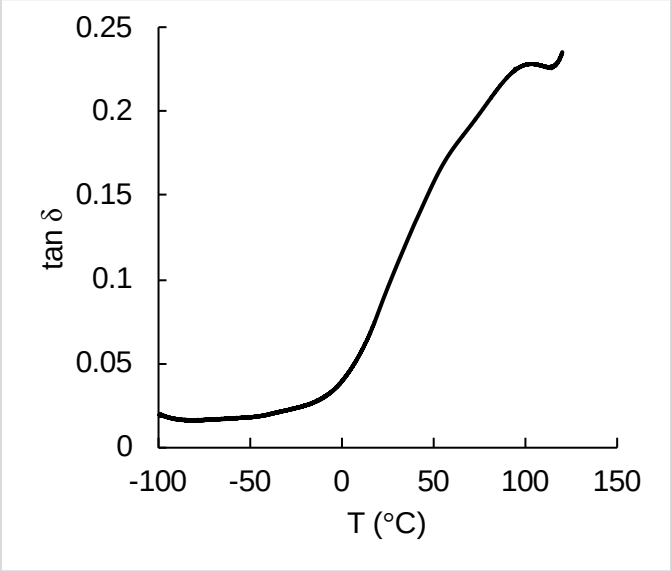

(b)

Figure 1. (a) Storage and loss moduli and (b) tan δ results for HDPE resin from DMA temperature sweep at 1 Hz.

The trends of *E"* with respect to temperature are presented in Figure 1a for HDPE resin. *E"* values extracted at three representative temperatures are presented in Table 1. The peak in *E"* at around 50°C corresponds to the α-relaxation in HDPE, which is associated with softening

of the interface between crystallites and the amorphous phase [50, 51]. Tan δ results are presented in Figure 1b and the values extracted at selected temperatures are presented in Table 1. This property, also known as the damping parameter, loss factor or loss tangent, is the ratio of the *E"* to *E'* and represents the relative magnitudes of the elastic and viscous behavior of the material. Previous studies have reported similar trends for *E'* and *E"* for polyethylene in the similar temperature range [50, 51]. Although no transition peaks are observed in the test temperature range used in this work, these previous studies have shown that α-, β-, and γ-transition peaks appear in the low temperature regions. These peaks correspond to relaxation of polymer chain and loss of crystallinity to form an amorphous phase. Increase in temperature from room temperature to higher temperatures results in decrease in *E'* and *E"* because of increase in polymer chain mobility. The damping parameter increases with increasing temperature over the range shown here as the elastic component of the response disappears as melting is approached while the viscous component remains.

3.1.2. Frequency sweep

In the second phase of DMA measurements, isothermal frequency sweeps are conducted in the range of temperatures from -10-120°C. A representative set of DMA curves obtained by varying frequency at various temperature steps for HDPE resin is shown in Figure 2. The trends show that *E'* increases with frequency, which indicates strain rate sensitivity in the material due to its viscoelastic nature. It is also observed that the frequency dependence of *E'* diminishes as temperature increases due to the increased resin flow characteristics. Similar results are also obtained on *E"* and tan δ during frequency sweep but the curves are not displayed here for brevity. The frequency sweep curves of *E'* are used to conduct TTS in order to construct master

curves that can provide frequency dependent *E'* of the material at a wider frequency range than that is used in the experimental testing. The master curve generated for a representative specimen of HDPE is shown in Figure 3. The reference temperature for this master curve is 25 °C. The plot is shown over a limited range of frequencies — the total range of frequencies from TTS is about 10^{-15}–10^{11} Hz. There are some kinks in the master curve at higher frequencies, which correspond to lower temperature data. This may be due to poor clamping of the specimen due to thermal contraction, causing slip at high (experimental) frequencies. Nevertheless, the curves superimpose well and so the TTS principle is expected to be appropriate for this data set.

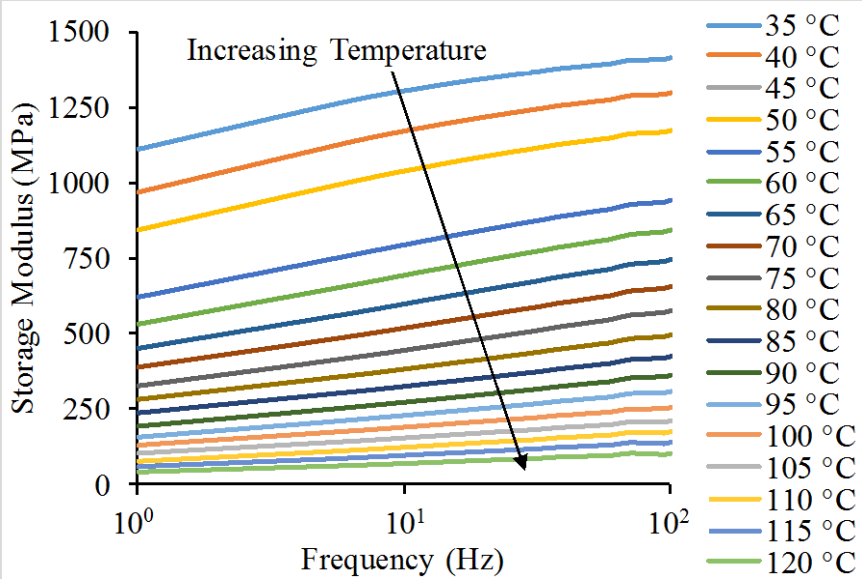

Figure 2. Representative data set from combined temperature-frequency sweep on a specimen of HDPE (showing only from 35 °C and above for clarity).

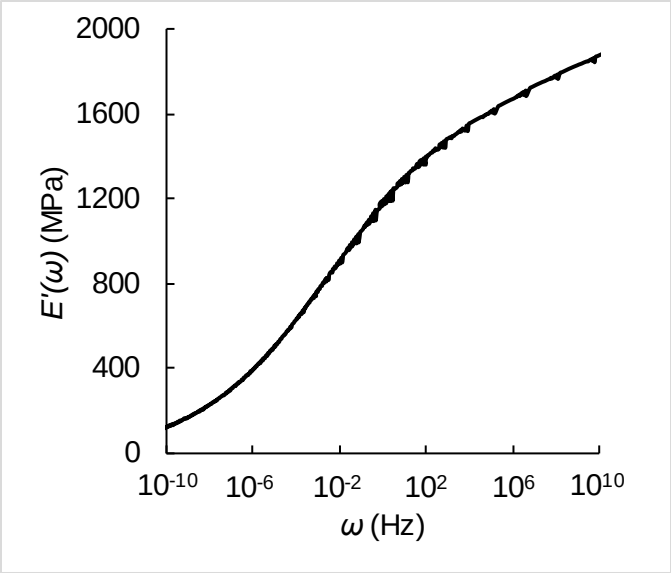

Figure 3. Master curve for HDPE at 25 °C.

3.2. HDPE/Fly Ash Syntactic Foams

3.2.1. Temperature Sweep

Results from the temperature sweep at 1 Hz are shown in Figure 4 and Figure 5 for HDPE20 and HDPE40, respectively. In both materials, a single peak in loss modulus is observed at 50 °C, which corresponds to the α-transition in the HDPE matrix. The edge of another peak is observed around -100 °C, which is the edge of the glass transition. The equipment used in the present work is not able to perform experiments much below this temperature, so the full glass transition for HDPE and its composites was not captured. Tan δ increases roughly linearly from 0 °C until melting. The peak in tan δ at melting observed in HDPE20 but missing in HDPE40 is only due to the stopping of the experiment very close to the melting temperature, which makes it very easy to stop the experiment before tan δ experiences this final rise. This peak is associated with melting and so has no bearing on the results of this work.

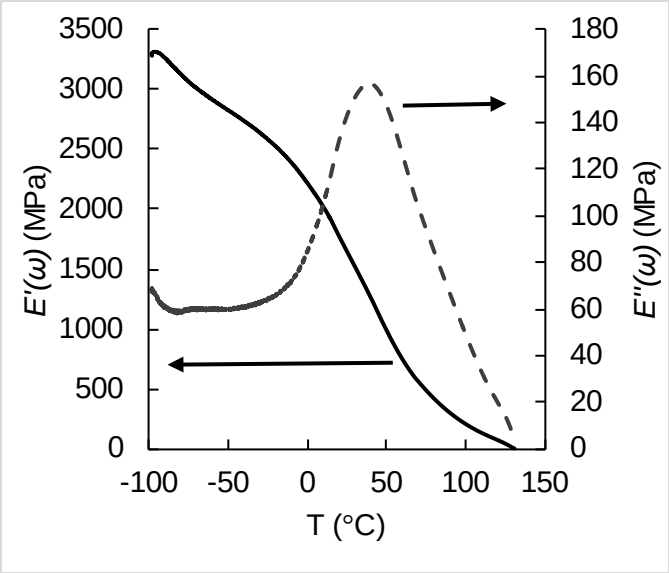

(a)

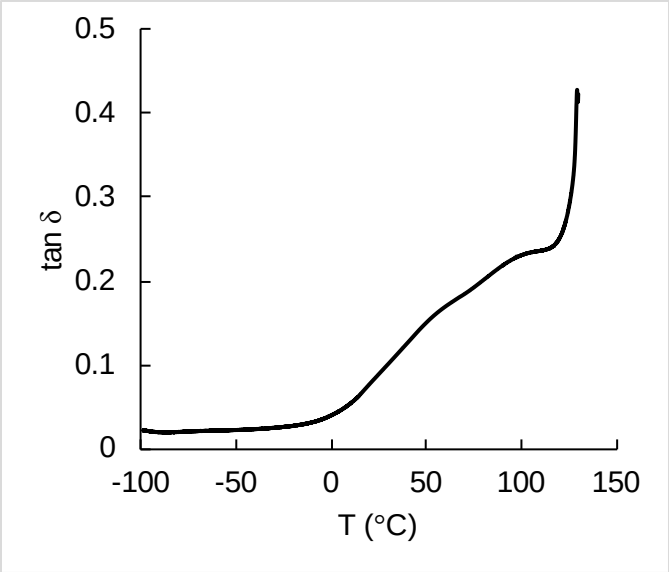

(b)

Figure 4. Temperature sweep results for HDPE20, showing (a) storage and loss moduli, and (b) tan δ as a function of temperature at 1 Hz.

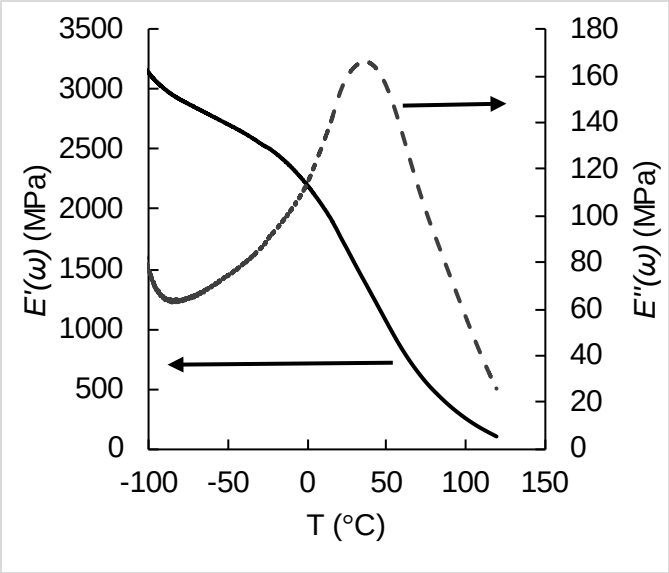

(a)

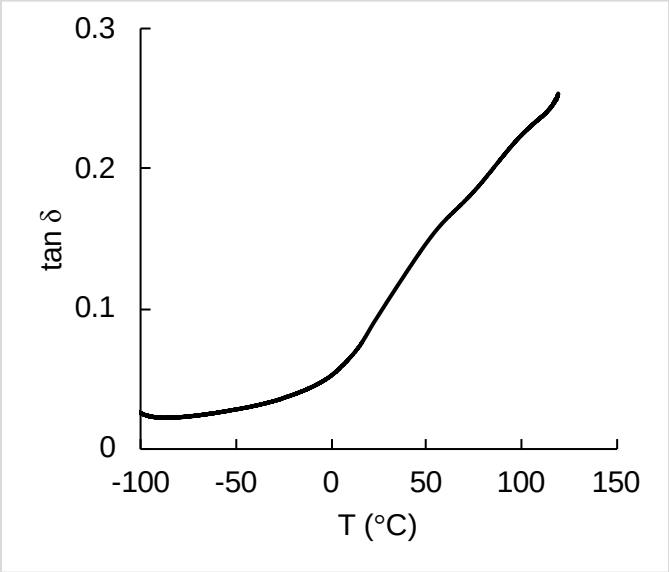

(b)

Figure 5. Temperature sweep results for HDPE40, showing (a) storage and loss moduli, and (b) tan δ as a function of temperature at 1 Hz.

3.2.2. Frequency Sweep

Frequency sweep results for HDPE20 and HDPE40 are shown in Figure 6 and Figure 7, respectively. The master curves generated from these sweeps are shown for both materials in Figure 8. As with neat HDPE, one transition is observed. The two syntactic foams have very

similar master curves. While it is normally expected that the addition of more stiff particles would increase the stiffness of the composite, breakage of the hollow particles during fabrication is significant in these types of syntactic foam. This causes a reduction in the reinforcing capability of the particles, leading to the less-than-expected modulus improvements [29]. The master curve for these materials cover about 27 decades of frequency.

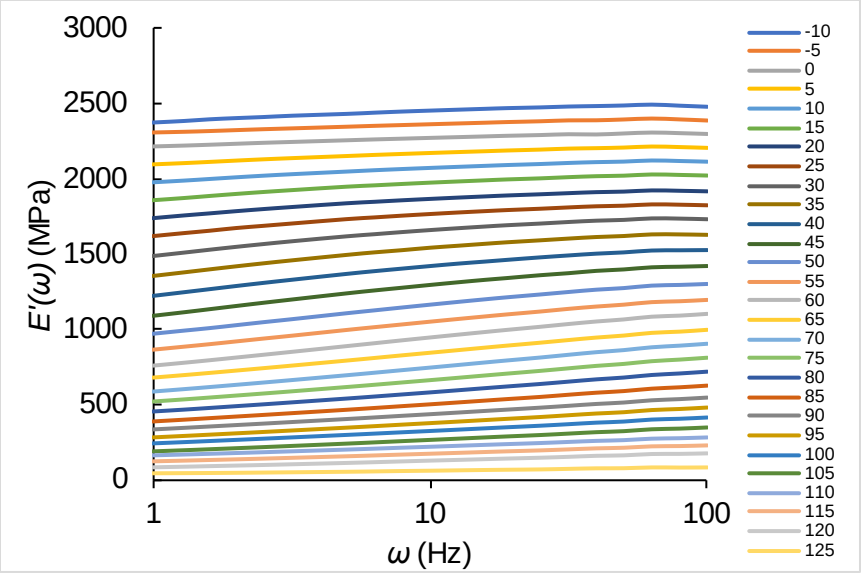

Figure 6. Frequency sweep results for HDPE20 syntactic foam.

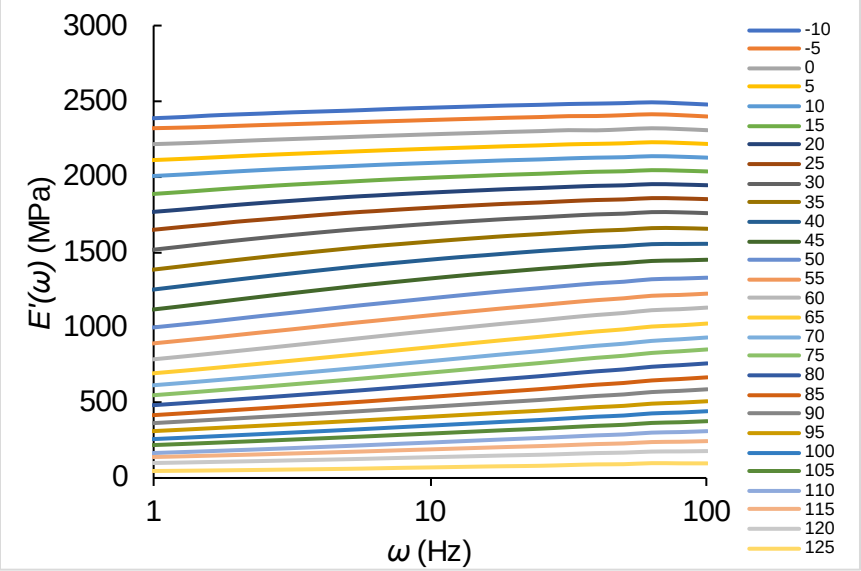

Figure 7. Frequency sweep results for HDPE40 syntactic foam.

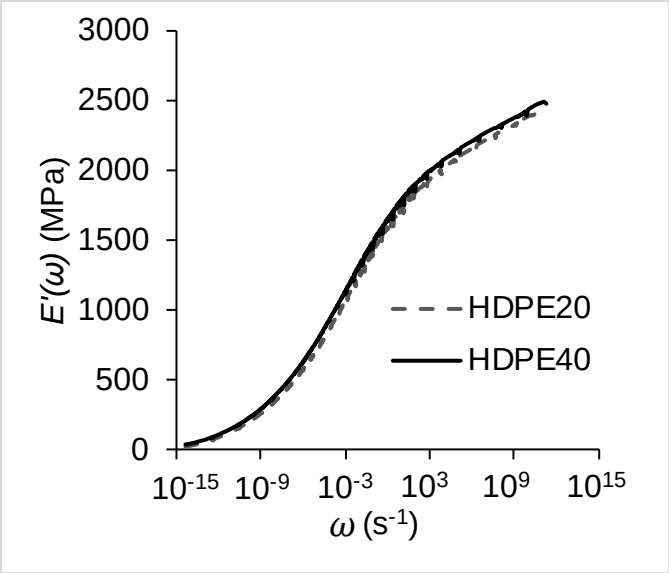

Figure 8. Master curves for HDPE/fly ash syntactic foams at 25 °C.

3.3. Vinyl ester

3.3.1. Temperature Sweep

Temperature sweep results for vinyl ester are shown in Figure 9. Two step transitions are observed in the sweep, and two corresponding peaks in the loss modulus are observed. The sharp glass transition is observed at around 125 °C and a broad β-transition is observed around 30 °C. The tail end of another transition may be occurring at -100 °C, though given the limitations of the equipment used it is not certain what this corresponds to. Regardless, such low temperature behavior is generally not an important factor in the time domain response at typically considered times and temperatures. This peak will likely not be observed at all in the frequency domain testing, because in that mode -10 °C is a practical limit of the equipment and even higher frequencies are unlikely to reveal this transition at that temperature.

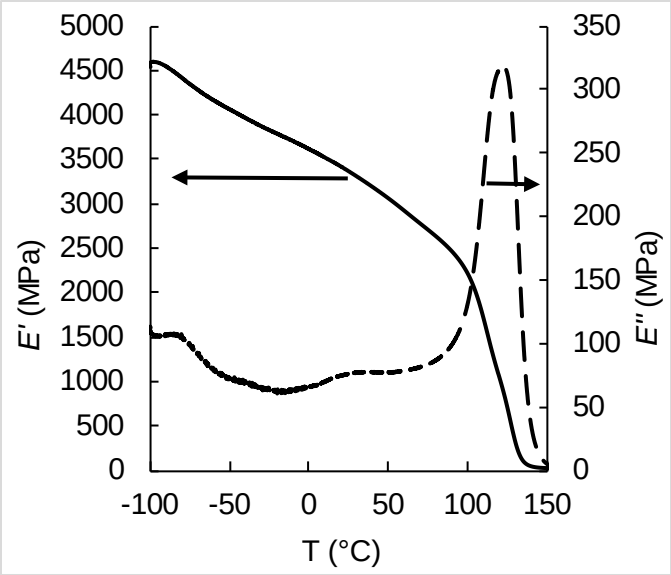

Figure 9. Temperature sweep results for vinyl ester.

3.3.2. Frequency Sweep

Frequency sweep results for vinyl ester are shown in Figure 10. The master curve resulting from shifting of this data around a reference temperature of 25 °C is shown in Figure 11. While it may appear that there is only one transition, we will find later that this data requires two transitions to obtain a satisfactory fit. This is also confirmed by the fact that in the temperature sweep, two peaks were observed in the loss modulus in this temperature range.

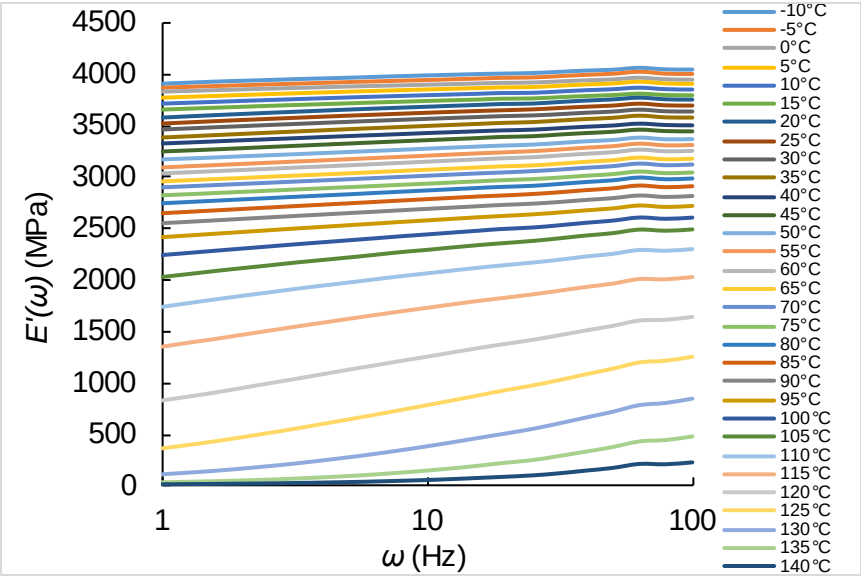

Figure 10. Frequency sweep results for vinyl ester.

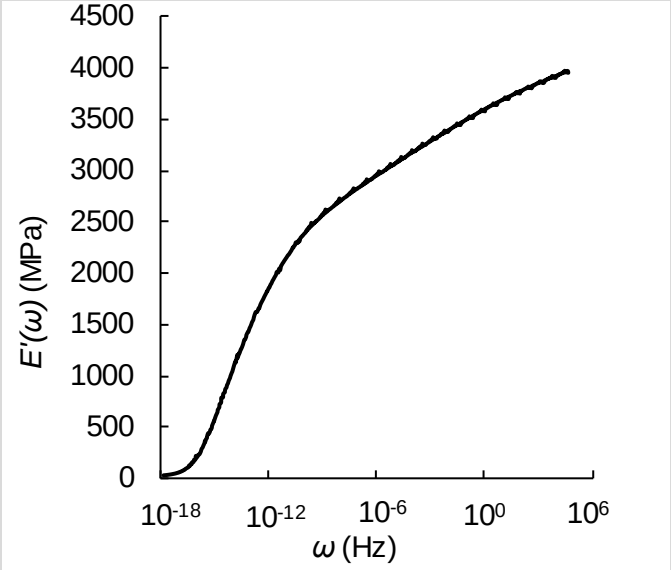

Figure 11. Master curve for vinyl ester at 25 °C.

CHAPTER 4. FREQUENCY TO TIME DOMAIN CONVERSION

4.1. Introduction

This section describes the procedure used in this work for transforming the frequency-domain data obtained from DMA into a time-domain form, and the use of that transformed material function for determining the response of the material to deformations at different strain rates. There is also some discussion of potential sources of error in the method. As an illustrative example, data from a previous publication [1] are included. Several intermediary steps and checks that are not described in detail for the materials tested in this work are shown here to give a complete picture of the method and its potential failings. The data presented here are for high density polyethylene, however the experiments were conducted only from room temperature and above and a slightly different clamping configuration was used (double cantilever). Regardless, the transformation technique is identical.

4.2. Time-temperature superposition

According to the TTS principle, the effects of temperature and frequency variations are interchangeable. This principle allows for the extension of data collected over a limited frequency domain to be expanded by many orders of magnitude by applying a shift factor on the data collected over a range of temperatures [52]. These curves are shifted to produce a master curve for the material based on a chosen reference temperature. Temperatures above the reference temperature shift to lower frequencies, while temperatures below shift to higher frequencies. These TTS shift factors are determined from the experimental data by shifting the curves obtained at different temperatures along the frequency axis to obtain a single smooth

master curve. The shift factors for most polymers have been found to obey the Williams-Landel-Ferry (WLF) equation [53]

$$\log_{10} a_T = \frac{-c_1(T - T_0)}{c_2 + T - T_0} \quad (1)$$

where a_T is the frequency shift factor, c_1 and c_2 are the WLF coefficients, T is the temperature each data set is acquired at, and T_0 is the reference temperature. Once the shift factors for a given material are determined, the corresponding WLF coefficients are independent of the choice of reference temperature. The values for c_1 and c_2 for HDPE are found to be 33±4 and 322±34 K, respectively, by fitting the WLF equation to the experimentally determined shift factors. The TTS parameters calculated for *E'* are also used for *E"* to construct master curves. The use of the same parameters to construct master curves provides validation for the values of these parameters. The shift factors for the virgin HDPE are similar to those reported in the literature [54]. However, direct comparison of the shift factors for virgin HDPE needs caution as they are affected by the degree of crystallinity and molecular weight.

The master curves for *E'* of HDPE resin at three arbitrarily selected reference temperatures are shown in Figure 12. The curves are shown in the frequency range 10^{-2}-10^{6} Hz, which is the range encountered in most vibration sensitive applications. However, the curves can be plotted for a much wider frequency range.

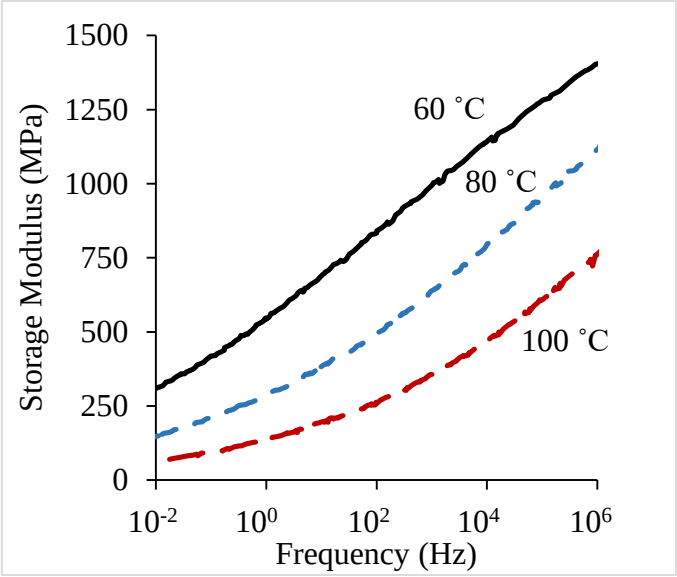

Figure 12. Time-temperature superposition results from DMA frequency sweep calculated for arbitrarily selected reference temperatures of 60, 80, and 100°C.

4.3. Transformation to time-domain

Using the TTS principle, *E'* and *E"* are found over a sufficiently wide range of frequencies that the information can be used to adequately characterize a viscoelastic function of the material. This frequency-domain viscoelastic function can, using an appropriate transformation, be converted to any of the other viscoelastic functions which may be more useful for engineering and design purposes. From *E'*, the time domain relaxation modulus $E(t)$ can be found using [55]

$$E(t) = \frac{2}{\pi}\int_0^\infty \frac{E'(\omega)}{\omega}\sin(\omega t)d\omega \tag{2}$$

where ω and t represent angular frequency and time, respectively. This is an improper integral, and so the storage modulus function must be known over an infinite range of frequencies. Since this is not possible by experimentation, we instead choose to extrapolate the measured data over this range. The central assumption of this procedure is that the storage modulus function

does not have any transformations outside the range observed by experiments. Thus, the estimated asymptotes of the storage modulus function by the extrapolating function are assumed to be the true ones. To extrapolate the experimental data in the frequency domain, the storage modulus master curve at a chosen temperature is fitted to a mixture of sigmoidal functions of $\log(\omega)$ of the form

$$E'(\omega) = c_1 + \sum_{j=1}^{N} c_{j1} \tanh(c_{j2} \log(\omega) + c_{j3}) \tag{3}$$

where the *c's* are the fit coefficients and $\log(\omega)$ is the natural logarithm. A fit of this form imposes that there are N smooth step transition in the storage modulus curve, each corresponding to a peak in E'', and that the behavior is asymptotic as frequency goes to zero or to positive infinity. For the experiments on HDPE, we observe one step in the storage modulus curve and so choose $N=1$. In such case, the fit function only satisfies the physically required positive and bounded behavior of the relaxation function at zero and infinite frequencies [55] if $c_1 > c_{11}$. However as the HDPE is above its T_g it behaves as a viscoelastic liquid and fitting of the data yields $c_1 \approx c_{11}$. The frequency at which $E'(\omega) = 0$ is of the order of 10^{-16}-10^{-17} Hz, which is sufficiently small that the negative E' will not affect the resulting relaxation function. For the fit to the experimental data, the R^2 value is above 0.999.

For other materials, N is chosen by observation of the loss modulus curve. Often transitions overlap on the storage modulus curve, while the peaks on the loss modulus curve can be more easily distinguished. There is no benefit in choosing a higher N than necessary, because it causes the fit to become poorly conditioned and is more likely to cause violation of the nonnegativity of the storage modulus at zero frequency.

The transform in Equation (2) of this fitting function is integrated numerically to yield the time domain relaxation function for the material. The relaxation function generated using the room temperature master curve is shown in Figure 13. The relaxation function can be observed to satisfy the requirements of fading memory and nonnegative stored and dissipated energy as expressed by [56]

$$E(t)\geq 0, \quad dE(t)/dt\leq 0, \quad d^2E(t)/dt^2\geq 0 \tag{4}$$

within the range of times displayed. Since $c_1<c_{11}$ in the fitted functions, at some time the relaxation function will violate the first condition and yield a negative value for $E(t)$. However, this crossover is observed to happen at around 10^{14} s (about 3 million years), well beyond practical time scales.

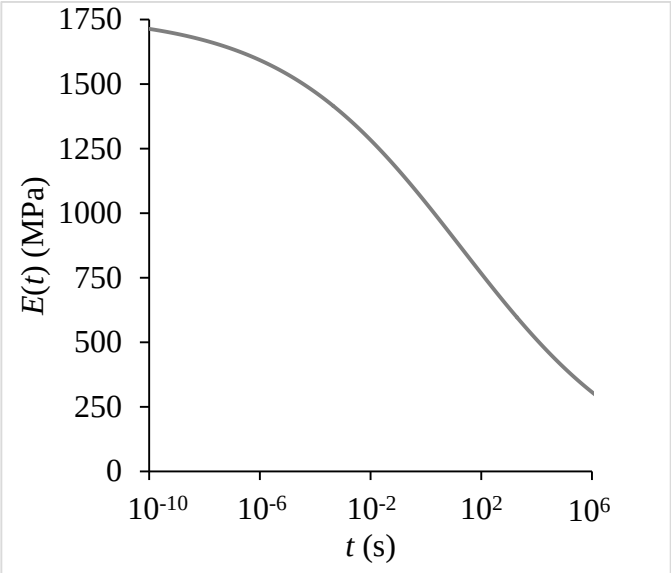

Figure 13. Time domain relaxation function determined using the transform in Equation (2) for HDPE.

The numerical integration of this transform is performed using the NDSolve command in Wolfram Mathematica 9. The integrand is the product of a strictly decreasing function

($E'(\omega)/\omega$ is guaranteed by the conditions on E' to be decreasing) with an oscillatory function. Thus, the integral can be approximated as an alternating series. The solver proceeds by using quadrature to integrate the function over the periods of the oscillatory part, which form the terms of the alternating sequence. An accelerated convergence algorithm, such as the Euler transform, is then used to estimate the infinite sum. The integral is estimated by this method for each time point of interest.

The relaxation modulus (also frequently referred to as the relaxation function) represents the stress history of the material when subjected to an infinite unitary strain. For an arbitrary strain history, the time-domain relaxation function determines the stress history according to [55]

$$\sigma(t) = E \times d\varepsilon = \int_{-\infty}^{t} E(t-\tau)\frac{d\varepsilon(\tau)}{d\tau}d\tau \tag{5}$$

where σ, ε and τ represent stress, strain and time variable used for integration, respectively. For constant strain rate deformation with a strain rate of $\dot{\varepsilon}$ beginning at $t=0$, which is the idealized deformation state in a standard tension test, the convolution integral simplifies to

$$\sigma(t) = \dot{\varepsilon}\int_{0}^{t} E(\tau)d\tau \tag{6}$$

Using this procedure, the linear viscoelastic stress-strain response of the materials can be predicted for any strain rate. To confirm the validity of the method, data for HDPE are compared with values found in the literature [57, 58] in Figure 14. The predictions of elastic modulus are evaluated as the secant modulus at 2.5% strain from the stress-stain values generated from the relaxation function, which is approximately the same as the definitions used in the literature. At strain rates of 10^{-5} to 4×10^{-2} s^{-1} the prediction from transformation of DMA results is in close agreement with the literature values, while at the strain rate of 4×10^{-1} s^{-1} the

prediction deviates by about 20% from the experiments. This deviation is further explored in the next step to determine if it is related to any experimental discrepancies or related to any parameters in the present calculation scheme.

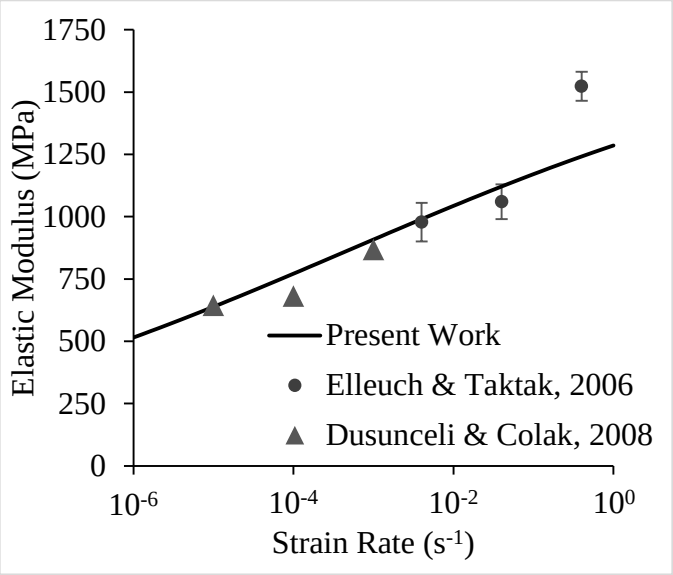

Figure 14. Comparison of modulus predictions from relaxation function with literature values for HDPE [57, 58]. The data in "Present Work" are taken from [1].

The accuracy of the time-domain relaxation function outside of the experimentally measured frequencies depends on the appropriateness of the fit function in the extrapolated regions. Therefore, the presence of additional transitions which are not measured experimentally will cause some deviation from the true relaxation function. When using the lowest temperature as the reference for the master curve, the maximum frequency of the TTS spectrum equals the maximum frequency attained in the experiment. Thus the upper limit for this data is 100 Hz when considering room temperature as the reference temperature. An approximation of the smallest time scale for which the relaxation function is corresponding to the experimental data can be attained according to [55]

$$t \to 2\pi/\omega \tag{7}$$

which yields a lower limit of 0.063 s. At times earlier than this the relaxation function is primarily influenced by the extrapolated values of the storage modulus curve which would correspond to lower temperature data. At a strain rate of 4×10^{-1} s^{-1}, a strain of 2.5% is reached in 0.0625 s, so that the data for 2.5% secant modulus at this and any higher strain rates is derived mainly from the extrapolation (though all times are affected to some extent by all frequencies, and vice versa). Since it is known that there are further transitions in the storage modulus curve below the lowest temperature measured in these experiments [50], without accounting for these transitions the relaxation function obtained here is an underestimate on shorter time scales. With one transition captured, the modulus-strain rate function (when plotted over a wider range of strain rates than in Figure 14) appears as a sigmoid. The missing transitions also lead to missing curvatures in the modulus-strain rate function. Thus for accurate high strain rate predictions, DMA frequency sweeps must be performed at temperatures below the reference temperature. This will yield data for higher frequencies in the shifted TTS domain.

Experimental measurement of higher strain rate properties is conducted by the split-Hopkinson pressure bar technique, which has been used to measure mechanical properties of materials at strain rates up to about 5×10^{3} s^{-1}. Deformation time scales obtained in those experiments are much smaller than the limit obtained by Equation 7 for the present data. For such case with multiple transitions, a similar fit function may be applied multiple times over successive frequency domains and integrated separately to yield the overall relaxation function, so long as each of the separate transforms is convergent. These predictions can be useful in mechanical and structural design as strain rate is an integral part of those calculations.

In the following chapter, three tasks are addressed: (a) experiments for HDPE are repeated using a lower starting temperature to determine if the deviations above can be mitigated, (b) the data is converted to a creep relaxation function to predict creep behavior of the material, and (c) the technique is validated for a polymer composite and for a thermoset resin.

CHAPTER 5. DISCUSSION

5.1. HDPE

Since the experiments in the previous work identified a limitation at higher strain rates, the first task is to investigate the means to correct this limitation. The data presented here were obtained following the recommendation of our previous work, namely that lower-temperature frequency sweeps should be included in the measurements to obtain higher frequencies in the TTS spectrum. The same transformation procedure, with *N=1*, was followed to obtain the results in this section.

5.1.1. Strain Rate Sensitivity

As observed in the master curve in Figure 3 for HDPE, which includes higher frequency data obtained from low temperature experiments, there is still only one observed transformation. Based on the prediction of the maximum accurate strain rate obtained in the previous chapter, the maximum strain rate for this data set is on the order of 10^{-10} s^{-1}. However, as shown in Figure 15, the data at 10^{-1} s^{-1} from the tension tests is still not in agreement with the prediction. Since variation in crystallinity can cause differences in both the measured mechanical properties and the dynamic mechanical behavior (especially the transition temperatures and therefore transition frequencies), study of HDPE under exactly the same processing conditions for both tension and dynamic mechanical experiments is likely needed to clarify the source of the deviation.

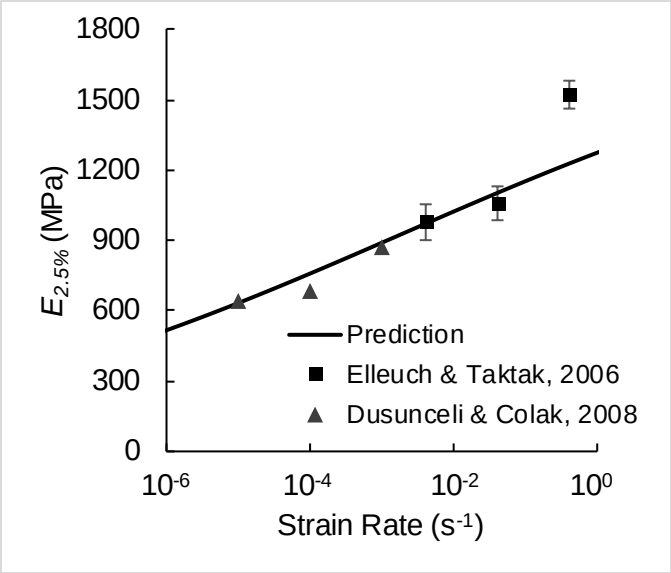

Figure 15. Comparison of predicted strain rate sensitivity of HDPE with values from the literature [57, 58].

5.1.2. Creep

Creep behavior of polymers is obviously an important concern for many applications. While it may appear at first inspection that the creep behavior can be obtained trivially by taking $E(t)^{-1}$, this is not the case and the relationship between the creep function $J(t)$ and the relaxation function is far more complicated. In Laplace domain, the relationship is

$$J = (s^2 E)^{-1} \tag{8}$$

where s is the Laplace frequency variable. While this form is compact, it is very difficult to evaluate the creep function through the Laplace transform. Instead, we can employ an approximate method given by Christensen [55, 59]

$$J(t) = \frac{E(t)}{E^2(t) + \frac{\pi^2 t^2}{4}\left\{\frac{dE(t)}{dt}\right\}^2} \tag{9}$$

which is easy to evaluate from the numerically obtained relaxation function. A similar integral to the convolution used in obtaining the stress history is used to obtain the creep strain history

for a given load. However, since we idealize creep as in instantaneous and maintained loading state, the creep function itself (multiplied by the applied stress) yields the creep strain history (i.e. the integral becomes a convolution with a Dirac delta, which simply returns the creep function).

Comparison of the creep predictions obtained in this work with experimental and modeling data reported by others [60, 61] is shown in Figure 16. The curve “Bozorg-Haddad 2011 Exp” is a year-long experimental study, while “Bozorg-Haddad 2011 TTS” is an accelerated test technique where the TTS principle is applied directly to shorter-time creep experiments conducted at different temperature. The “Chevali fit” curve represents a nonlinear model developed by the authors, based off a power law model. Data for the fit were obtained though TTS and variation of the stress. Good agreement between all the predictions and the experiments is seen at up to one year. Beyond that, the predictions from the current work follow the nonlinear fit but deviate from the TTS predictions of Bozorg-Haddad et al. Since no direct experimental data is available at these time scales for HDPE, it is difficult to assess which method is valid in this time frame. However, it is noted that the DMA transform method of this work is the conservative if used in design, i.e. it predicts higher strain and faster creep than the experimental studies, and so is potentially safe to use as an upper bound. Further, the presence of a turning point simplifies calculation of a single nominal maximum creep life.

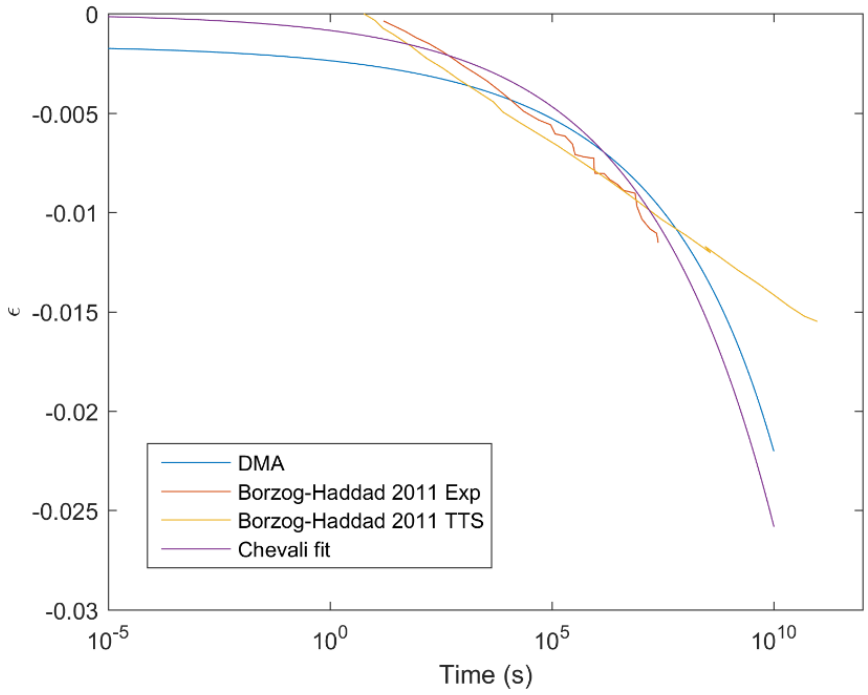

Figure 16. Comparison of creep predictions with literature values [60, 61].

5.2. HDPE/Fly Ash

Using the transformation technique of this work, the strain rate sensitivity predictions obtained for HDPE/fly ash syntactic foams are shown in Figure 17. Excellent agreement is observed between the modulus measured by tension testing and the predictions. The data for this section are all evaluated as the secant modulus at 0.5% strain, since the present of the hollow particles significantly reduces the ductility of the composites [30, 48, 62] and fracture occurs at as low as 1% strain. The tensile data for these composites is not available at higher strain rates, so it is left unknown what is the upper limit of the accuracy of the prediction. Measurement at higher strain rates is complicated by the brittleness of the material, which is likely worsened at higher strain rates due to a ductile-to-brittle transition [49].

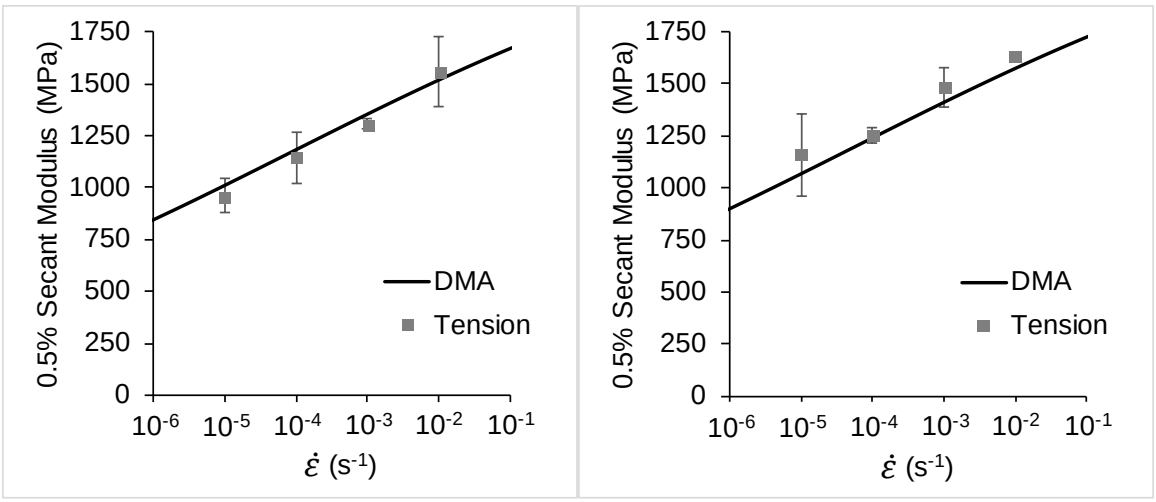

Figure 17. Strain rate sensitivity of HDPE/fly ash syntactic foams containing (a) 20 wt.% and (b) 40 wt.% cenospheres.

5.3. Vinyl Ester

Predictions of the strain rate sensitivity of vinyl ester are shown in Figure 18. Again, the modulus is estimated as the 0.5% secant. Vinyl ester is a thermoset, and shows significantly less strain rate sensitivity and has a fairly linear elastic initial region. As observed in the figure, the strain rate sensitivity is not very strong. This is reflected in the prediction from the DMA transform method, which shows slightly increasing modulus with increasing strain rate. This case is a good illustration of the fact that in general, storage modulus cannot be used as a direct measure of the material's elastic modulus, because even in cases with little strain rate sensitivity observable from tension results there is still an effect. Using storage modulus values directly would thus yield an incorrect measure of the material stiffness.

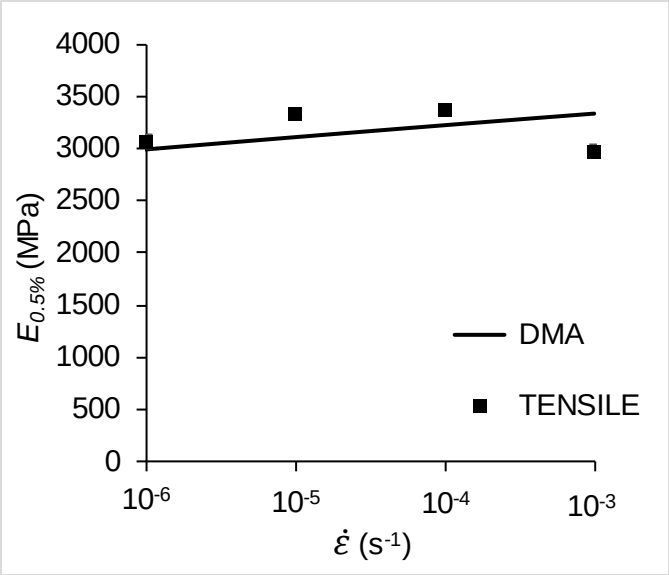

Figure 18. Strain rate sensitivity of vinyl ester compared to tensile experiments (error bars are smaller than the points on the plot).

CHAPTER 6. CONCLUSIONS

A scheme is presented to convert the storage modulus and loss modulus results obtained from dynamic mechanical analysis (DMA) to elastic modulus values at different strain rates. Validation of the technique is presented for HDPE, HDPE/fly ash syntactic foams, and for vinyl ester resin. Guidelines are presented to define the domain in which the prediction scheme is expected to work for polymers.

Using the TTS principle, the limited set of results obtained from DMA are expanded around a single temperature to cover a much wider range of frequencies. This frequency spectrum is then inverted to the time-domain relaxation function, which can yield accurate predictions of the linear viscoelastic response of the materials. The following conclusions are drawn from the work:

- The transform technique is valid over a wide range of strain rates (at least 4 decades) for all the material systems tested. The technique is validated for a thermoplastic, a thermoplastic-matrix composite, and a thermoset resin.
- At higher strain rates, predictions for HDPE were observed to deviate from the predictions of the transform. Inclusion of data from additional temperatures is not sufficient to improve the prediction and obtain matching with the experimental data.
- Conversion to a creep relaxation function by an approximate method is possible, and yields estimates that are in good agreement with the available experimental data.

CHAPTER 7. REFERENCES

1. Zeltmann, S.E., Kumar, B.B., Doddamani, M., and Gupta, N., *Prediction of strain rate sensitivity of high density polyethylene using integral transform of dynamic mechanical analysis data.* Polymer, 2016. **101**: p. 1-6.
2. Phan, V.T., Choqueuse, D., Cognard, J.Y., and Sohier, L., *Experimental analysis and modelling of the long term thermo-mechanical behaviour of glass/polypropylene syntactic used on thermally insulated offshore pipeline.* Progress in Organic Coatings, 2013. **76**(2–3): p. 341-350.
3. Shunmugasamy, V.C., Pinisetty, D., and Gupta, N., *Viscoelastic properties of hollow glass particle filled vinyl ester matrix syntactic foams: effect of temperature and loading frequency.* Journal of Materials Science, 2013. **48**(4): p. 1685-1701.
4. Haines, P.J., *Thermal methods of analysis: principles, applications and problems*. 2012: Springer Science & Business Media.
5. Menard, K.P., *Dynamic mechanical analysis: a practical introduction*. 2008: CRC press.
6. Kloosterboer, J.G. and Lijten, G.F.C.M., *Thermal and mechanical analysis of a photopolymerization process.* Polymer, 1987. **28**(7): p. 1149-1155.
7. Calleja, G., Jourdan, A., Ameduri, B., and Habas, J.-P., *Where is the glass transition temperature of poly(tetrafluoroethylene)? A new approach by dynamic rheometry and mechanical tests.* European Polymer Journal, 2013. **49**(8): p. 2214-2222.

8. Rieger, J., *The glass transition temperature Tg of polymers—Comparison of the values from differential thermal analysis (DTA, DSC) and dynamic mechanical measurements (torsion pendulum).* Polymer Testing, 2001. **20**(2): p. 199-204.

9. Ning, X. and Ishida, H., *Phenolic materials via ring-opening polymerization of benzoxazines: Effect of molecular structure on mechanical and dynamic mechanical properties.* Journal of Polymer Science Part B: Polymer Physics, 1994. **32**(5): p. 921-927.

10. Wang, H., Aubuchon, S.R., Thompson, D.G., Osborn, J.C., Marsh, A.L., Nichols, W.R., Schoonover, J.R., and Palmer, R.A., *Temperature-Dependent Dynamic Mechanical Analysis−Fourier Transform Infrared Study of a Poly(ester urethane) Copolymer.* Macromolecules, 2002. **35**(23): p. 8794-8801.

11. Delebecq, E., Hermeline, N., Flers, A., and Ganachaud, F., *Looking over Liquid Silicone Rubbers: (2) Mechanical Properties vs Network Topology.* ACS Applied Materials & Interfaces, 2012. **4**(7): p. 3353-3363.

12. Jose, S., Thomas, S., Parameswaranpillai, J., Aprem, A.S., and Karger-Kocsis, J., *Dynamic mechanical properties of immiscible polymer systems with and without compatibilizer.* Polymer Testing, 2015. **44**: p. 168-176.

13. Ljungberg, N. and Wesslén, B., *The effects of plasticizers on the dynamic mechanical and thermal properties of poly(lactic acid).* Journal of Applied Polymer Science, 2002. **86**(5): p. 1227-1234.

14. Jones, D.S., *Dynamic mechanical analysis of polymeric systems of pharmaceutical and biomedical significance.* International Journal of Pharmaceutics, 1999. **179**(2): p. 167-178.

15. Kostka, P., Holeczek, K., Höhne, R., Filippatos, A., and Modler, N., *Extension and application of dynamic mechanical analysis for the estimation of spatial distribution of material properties.* Polymer Testing, 2016. **52**: p. 184-191.

16. Manikandan Nair, K.C., Thomas, S., and Groeninckx, G., *Thermal and dynamic mechanical analysis of polystyrene composites reinforced with short sisal fibres.* Composites Science and Technology, 2001. **61**(16): p. 2519-2529.

17. Saba, N., Jawaid, M., Alothman, O.Y., and Paridah, M.T., *A review on dynamic mechanical properties of natural fibre reinforced polymer composites.* Construction and Building Materials, 2016. **106**: p. 149-159.

18. Aurilia, M., Piscitelli, F., Sorrentino, L., Lavorgna, M., and Iannace, S., *Detailed analysis of dynamic mechanical properties of TPU nanocomposite: The role of the interfaces.* European Polymer Journal, 2011. **47**(5): p. 925-936.

19. Bansal, A., Yang, H., Li, C., Cho, K., Benicewicz, B.C., Kumar, S.K., and Schadler, L.S., *Quantitative equivalence between polymer nanocomposites and thin polymer films.* Nat Mater, 2005. **4**(9): p. 693-698.

20. Jin, Z., Pramoda, K.P., Xu, G., and Goh, S.H., *Dynamic mechanical behavior of melt-processed multi-walled carbon nanotube/poly(methyl methacrylate) composites.* Chemical Physics Letters, 2001. **337**(1–3): p. 43-47.

21. Lozano, K. and Barrera, E.V., *Nanofiber-reinforced thermoplastic composites. I. Thermoanalytical and mechanical analyses.* Journal of Applied Polymer Science, 2001. **79**(1): p. 125-133.

22. Mahdi, E.M. and Tan, J.-C., *Dynamic molecular interactions between polyurethane and ZIF-8 in a polymer-MOF nanocomposite: Microstructural, thermo-mechanical and viscoelastic effects.* Polymer, 2016. **97**: p. 31-43.

23. Ramanathan, T., Abdala, A.A., StankovichS, Dikin, D.A., Herrera Alonso, M., Piner, R.D., Adamson, D.H., Schniepp, H.C., Chen, X., Ruoff, R.S., Nguyen, S.T., Aksay, I.A., Prud'Homme, R.K., and Brinson, L.C., *Functionalized graphene sheets for polymer nanocomposites.* Nat Nano, 2008. **3**(6): p. 327-331.

24. Yang, S., Taha-Tijerina, J., Serrato-Diaz, V., Hernandez, K., and Lozano, K., *Dynamic mechanical and thermal analysis of aligned vapor grown carbon nanofiber reinforced polyethylene.* Composites Part B: Engineering, 2007. **38**(2): p. 228-235.

25. Ago, M., Jakes, J.E., and Rojas, O.J., *Thermomechanical Properties of Lignin-Based Electrospun Nanofibers and Films Reinforced with Cellulose Nanocrystals: A Dynamic Mechanical and Nanoindentation Study.* ACS Applied Materials & Interfaces, 2013. **5**(22): p. 11768-11776.

26. Yoonessi, M., Lebrón-Colón, M., Scheiman, D., and Meador, M.A., *Carbon Nanotube Epoxy Nanocomposites: The Effects of Interfacial Modifications on the Dynamic Mechanical Properties of the Nanocomposites.* ACS Applied Materials & Interfaces, 2014. **6**(19): p. 16621-16630.

27. Park, S. and Kim, Y., *Interconversion between Relaxation Modulus and Creep Compliance for Viscoelastic Solids.* Journal of Materials in Civil Engineering, 1999. **11**(1): p. 76-82.

28. Gross, B., *Mathematical structure of the theories of viscoelasticity*. Vol. 1190. 1953, Paris: Hermann.

29. Bharath Kumar, B.R., Doddamani, M., Zeltmann, S.E., Gupta, N., Uzma, Gurupadu, S., and Sailaja, R.R.N., *Effect of particle surface treatment and blending method on flexural properties of injection-molded cenosphere/HDPE syntactic foams.* Journal of Materials Science, 2016. **51**(8): p. 3793-3805.

30. Bharath Kumar, B.R., Doddamani, M., Zeltmann, S.E., Gupta, N., Ramesh, M.R., and Ramakrishna, S., *Processing of cenosphere/HDPE syntactic foams using an industrial scale polymer injection molding machine.* Materials & Design, 2016. **92**: p. 414-423.

31. Gupta, N., Zeltmann, S., Shunmugasamy, V., and Pinisetty, D., *Applications of Polymer Matrix Syntactic Foams.* JOM, 2013: p. 1-10.

32. Gupta, N., Pinisetty, D., and Shunmugasamy, V.C., *Reinforced Polymer Matrix Syntactic Foams : Effect of Nano and Micro-Scale Reinforcement*. 2013, Cham: Springer International Publishing.

33. Yalcin, B., *Chapter 7 - Hollow Glass Microspheres in Polyurethanes*, in *Hollow Glass Microspheres for Plastics, Elastomers, and Adhesives Compounds*, S.E. Amos and B. Yalcin, Editors. 2015, William Andrew Publishing (Elsevier): Oxford. p. 175-200.

34. Yalcin, B. and Amos, S.E., *Chapter 3 - Hollow Glass Microspheres in Thermoplastics*, in *Hollow Glass Microspheres for Plastics, Elastomers, and Adhesives Compounds*, S.E. Amos and B. Yalcin, Editors. 2015, William Andrew Publishing (Elsevier): Oxford. p. 35-105.

35. Bachmatiuk, A., Börrnert, F., Schäffel, F., Zaka, M., Martynkowa, G.S., Placha, D., Schönfelder, R., Costa, P.M.F.J., Ioannides, N., Warner, J.H., Klingeler, R., Büchner,

B., and Rümmeli, M.H., *The formation of stacked-cup carbon nanotubes using chemical vapor deposition from ethanol over silica.* Carbon, 2010. **48**(11): p. 3175-3181.

36. Alkan, C., Arslan, M., Cici, M., Kaya, M., and Aksoy, M., *A study on the production of a new material from fly ash and polyethylene.* Resources, Conservation and Recycling, 1995. **13**(3–4): p. 147-154.

37. Li, J., Agarwal, A., Iveson, S.M., Kiani, A., Dickinson, J., Zhou, J., and Galvin, K.P., *Recovery and concentration of buoyant cenospheres using an Inverted Reflux Classifier.* Fuel Processing Technology, 2014. **123**: p. 127-139.

38. Lauf, R.J., *Cenospheres in fly ash and conditions favouring their formation.* Fuel, 1981. **60**(12): p. 1177-1179.

39. Anshits, N.N., Mikhailova, O.A., Salanov, A.N., and Anshits, A.G., *Chemical composition and structure of the shell of fly ash non-perforated cenospheres produced from the combustion of the Kuznetsk coal (Russia).* Fuel, 2010. **89**(8): p. 1849-1862.

40. Gupta, N., Singh Brar, B., and Woldesenbet, E., *Effect of filler addition on the compressive and impact properties of glass fibre reinforced epoxy.* Bulletin of Materials Science, 2001. **24**(2): p. 219-223.

41. Satapathy, B., Das, A., and Patnaik, A., *Ductile-to-brittle transition in cenosphere-filled polypropylene composites.* Journal of Materials Science, 2011. **46**(6): p. 1963-1974.

42. Qiao, J. and Wu, G., *Tensile properties of fly ash/polyurea composites.* Journal of Materials Science, 2011. **46**(11): p. 3935-3941.

43. Manakari, V., Parande, G., Doddamani, M., Gaitonde, V.N., Siddhalingeshwar, I.G., Kishore, Shunmugasamy, V.C., and Gupta, N., *Dry sliding wear of epoxy/cenosphere syntactic foams.* Tribology International, 2015. **92**: p. 425-438.

44. Labella, M., Zeltmann, S.E., Shunmugasamy, V.C., Gupta, N., and Rohatgi, P.K., *Mechanical and thermal properties of fly ash/vinyl ester syntactic foams.* Fuel, 2014. **121**: p. 240-249.

45. Hossain, M.M. and Shivakumar, K., *Compression fatigue performance of a fire resistant syntactic foam.* Composite Structures, 2011. **94**(1): p. 290-298.

46. Doddamani, M., Kishore, Shunmugasamy, V.C., Gupta, N., and Vijayakumar, H.B., *Compressive and flexural properties of functionally graded fly ash cenosphere–epoxy resin syntactic foams.* Polymer Composites, 2015. **36**(4): p. 685-693.

47. Bharath Kumar, B.R., Doddamani, M., Zeltmann, S.E., Gupta, N., Uzma, Gurupadu, S., and Sailaja, R.R.N., *Effect of surface treatment and blending method on flexural properties of injection molded cenosphere/HDPE syntactic foams.* Journal of Materials Science, 2015. **51**(8): p. 3793-3805.

48. Bharath Kumar, B.R., Zeltmann, S.E., Doddamani, M., Gupta, N., Uzma, Gurupadu, S., and Sailaja, R.R.N., *Effect of cenosphere surface treatment and blending method on the tensile properties of thermoplastic matrix syntactic foams.* Journal of Applied Polymer Science, 2016: p. 43881.

49. Bharath Kumar, B.R., Singh, A.K., Doddamani, M., Luong, D.D., and Gupta, N., *Quasi-Static and High Strain Rate Compressive Response of Injection-Molded Cenosphere/HDPE Syntactic Foam.* JOM, 2016: p. 1-11.

50. Khanna, Y.P., Turi, E.A., Taylor, T.J., Vickroy, V.V., and Abbott, R.F., *Dynamic mechanical relaxations in polyethylene.* Macromolecules, 1985. **18**(6): p. 1302-1309.

51. Khonakdar, H., Morshedian, J., Wagenknecht, U., and Jafari, S., *An investigation of chemical crosslinking effect on properties of high-density polyethylene.* Polymer, 2003. **44**(15): p. 4301-4309.

52. Ferry, J.D., *Viscoelastic Properties of Polymers*. 1961, New York: John Wiley & Sons, Inc.

53. Williams, M.L., Landel, R.F., and Ferry, J.D., *The Temperature Dependence of Relaxation Mechanisms in Amorphous Polymers and Other Glass-forming Liquids.* Journal of the American Chemical Society, 1955. **77**(14): p. 3701-3707.

54. Gol'dman, A.Y. and Grinman, A.M., *Variant of time-temperature superposition for partially crystalline polymers (high-density polyethylene).* Polymer Mechanics, 1974. **10**(2): p. 224-230.

55. Christensen, R.M., *Theory of Viscoelasticity: An Intoduction*. 1982, New York: Academic Press.

56. Christensen, R.M., *Restrictions Upon Viscoelastic Relaxation Functions and Complex Moduli.* Transactions of The Society of Rheology, 1972. **16**(4): p. 603-614.

57. Dusunceli, N. and Colak, O.U., *The effects of manufacturing techniques on viscoelastic and viscoplastic behavior of high density polyethylene (HDPE).* Materials & Design, 2008. **29**(6): p. 1117-1124.

58. Elleuch, R. and Taktak, W., *Viscoelastic behavior of HDPE polymer using tensile and compressive loading.* Journal of Materials Engineering and Performance, 2006. **15**(1): p. 111-116.

59. Park, S.W. and Kim, Y.R., *Interconversion between Relaxation Modulus and Creep Compliance for Viscoelastic Solids.* Journal of Materials in Civil Engineering, 1999. **11**(1).

60. Bozorg-Haddad, A. and Iskander, M., *Comparison of Accelerated Compressive Creep Behavior of Virgin HDPE Using Thermal and Energy Approaches.* Journal of Materials Engineering and Performance, 2011. **20**(7): p. 1219-1229.

61. Chevali, V.S., Dean, D.R., and Janowski, G.M., *Flexural creep behavior of discontinuous thermoplastic composites: Non-linear viscoelastic modeling and time–temperature–stress superposition.* Composites Part A: Applied Science and Manufacturing, 2009. **40**(6–7): p. 870-877.

62. Bharath Kumar, B.R., Doddamani, M., Zeltmann, S.E., Gupta, N., Ramesh, M.R., and Ramakrishna, S., *Data characterizing tensile behavior of censophere/HDPE syntactic foam.* Data in Brief, 2015. **6**: p. 933-941.